

# Kinetics of nucleation and halt-in-growth processes in a thin layer

T. TAGAMI\*, S.-I. TANAKA

Tanaka Solid Junction Project, ERATO, Japan Science and Technology Corporation, 1-1-1, Fukuura, Kanazawa-ku, Yokohama 236, Japan

The methods of determining the kinetic exponents in the equation,  $dX/dV_{\text{ex}} = (1 - X)^{2-\gamma}$ , used for nucleation and halt-in-growth processes where  $X$  is the transformed fraction,  $V_{\text{ex}}$  the KJMA extended volume fraction which is related to time  $t$ , and  $\gamma$  is the overlap factor which accounts for the overlap between a crystallite and a phantom crystallite, are presented. The applications of the Kolmogorov–Johnson–Mehl–Avrami plot ( $\gamma = 1$ ) and the Austin–Rickett plot ( $\gamma = 0$ ) to this process are inappropriate, because the overlap factor is  $0 < \gamma < 1$ . The impingement exponent  $2-\gamma$  and the time exponent are determined from the linear relation of  $\ln\{(1 - X)^{\gamma-1} - 1\}/(1 - \gamma)$  versus  $\ln t$ . From the value of  $\gamma$ , the crystal shape and growth dimension can be estimated by referring to the mathematical value of  $\gamma$ . The methods of evaluating the activation energy,  $Q$ , are presented using the Arrhenius relation. The value of  $Q$  is not directly related to the overlap factor  $\gamma$ ; however,  $\gamma$  appears as a constant term in the expression for  $Q$ . © 1999 Kluwer Academic Publishers

## 1. Introduction

Various isothermal transformations have been described by the Kolmogorov–Johnson–Mehl–Avrami (KJMA) equation [1–5] and the Austin–Rickett (AR) equation [6]. In these equations, the transformed fraction,  $X$ , at time  $t$  is generally expressed as

$$\frac{dX}{dt} = Bt^{n-1}(1 - X)^i \quad (1)$$

where  $B$  is a model-dependent factor,  $n$  is a time exponent and  $i$  is unity (KJMA) or 2 (AR). The factor  $(1 - X)^i$  is referred to as the impingement factor, and is commonly used to correct for the effects of such factors as the impingement of crystallites and the depletion of the untransformed matrix in solute content [7, 8].

The time exponent,  $n$ , is calculated from the experimental data of  $X$  using the KJMA equation or the AR equation. The activation energy,  $Q$ , is also evaluated using the Arrhenius relation. Furthermore, these equations have been employed in studies of non-isothermal transformation kinetics [9–11]. Although a large number of studies have been made on the evaluation of  $n$  and  $Q$  using the KJMA equation ( $i = 1$ ) and the AR equation ( $i = 2$ ), little is known about  $n$  and  $Q$  when the impingement exponent is  $1 < i < 2$ .

Recently, we have noted a limitation of the KJMA and AR models when the crystal growth stops at a fixed size [12–15]: in a thin amorphous silicon (a-Si) layer, the crystal growth stops between two amorphous silicon oxide interfaces [16, 17]. A similar limitation of silicon

crystal growth between interfaces has been reported for the laser-annealed a-Si/amorphous silicon nitride multilayered structure [18, 19]. This structure exhibits visible photoluminescence from silicon nanocrystals and could be used in optoelectric applications.

When the crystal growth stops at a fixed size, phantom crystallites, which are grown from phantom nuclei [4], partly protrude beyond the crystallites. This causes a serious problem in that the transformed fraction is overestimated by the protruding phantom crystallites. Then, phantom crystallites are shrunk to an effective size to correct the transformed fraction. In our previous paper [14], a mathematical model was successfully used to deal with the effective size using the factor  $\gamma$  which accounts for the overlap between a phantom crystallite and a crystallite. This model leads to the equation

$$\frac{dX}{dV_{\text{ex}}} = (1 - X)^{2-\gamma} \quad (2)$$

where  $V_{\text{ex}}$  is the KJMA extended volume fraction which can be related to time. An equation of this form has long been known as the phenomenological equation for non-random impingement [7, 20].

The impingement exponent is expressed as  $1 < (2 - \gamma) < 2$  because  $\gamma$  ranges from 1–0. The explicit value of  $\gamma$  can be derived from the crystal shape and the growth dimension [12], for example,  $\gamma = 3/4$  for needle-shaped crystallites in one dimension,  $\gamma = 1 - 3^{3/2}/4\pi$  for circular crystallites in two dimensions,

\* Present address: Tsukuba Research Centre, Technical Research Laboratory, Nippon Sheet Glass Co., Ltd, 5-4 Tokodai, Tsukuba, Ibaraki 300-26, Japan.

and  $\gamma = 15/32$  for spherical crystallites in three dimensions. The transformation kinetics for the half-in-growth, however, has never been reported.

In this paper, we focus on the effect of the overlap factor  $\gamma$  on the evaluation of the time exponent,  $n$ , and the activation energy  $Q$ .

## 2. Exponents in the present kinetic equation

In this section, the time exponent,  $n$ , and the impingement exponent,  $(2-\gamma)$ , in the present kinetic equation are evaluated.

We assume the following nucleation and growth process [13].

1. Nucleation sites are randomly formed in space at a rate of  $N(t)$  per unit volume.

2. Nuclei grow instantaneously to a fixed size  $k$  and then stop growing.

This process is referred to as the ‘‘present process’’.

### 2.1. Time exponent in the KJMA plot

The time exponent,  $n$ , is evaluated from the KJMA plot to clarify the effect of the overlap factor,  $\gamma$ , on the KJMA plot. From the present nucleation and growth assumption, the KJMA extended volume fraction is given by

$$V_{\text{ex}} = k \int_0^t N(t') dt' \quad (3)$$

If the KJMA model ( $\gamma = 1$ ) were applied to the present process, the transformed fraction,  $X_{\text{KJMA}}$ , would be expressed as

$$X_{\text{KJMA}} = 1 - \exp(-V_{\text{ex}}) \quad (4)$$

The time exponent,  $n$ , in the KJMA model at a constant nucleation rate,  $N(t) = N$ , is then given by unity, because a plot of  $\ln[-\ln(1 - X_{\text{KJMA}})]$  versus  $\ln t$  results in a slope of unity. The KJMA model then yields  $n = 1$  with  $\gamma = 1$ .

From Equations 2 and 3, the transformed fraction in the present model is given by

$$X = 1 - [1 + (1 - \gamma)V_{\text{ex}}]^{1/(\gamma-1)} \quad (5)$$

Using the KJMA plot, the time exponent,  $n$ , is expressed as

$$n = \frac{d \ln[-\ln(1 - X)]}{d \ln V_{\text{ex}}} = \left[ \frac{(1 - \gamma)V_{\text{ex}}}{\ln[1 + (1 - \gamma)V_{\text{ex}}]} \right] \left[ \frac{1}{1 + (1 - \gamma)V_{\text{ex}}} \right] \quad (6)$$

Thus  $n$  is a function of only the product  $(1 - \gamma)V_{\text{ex}}$ . At the beginning of the transformation ( $V_{\text{ex}} \rightarrow 0$ ),  $n$  is unity because  $n$  is approximated to  $1/[1 + (1 - \gamma)V_{\text{ex}}]$  for  $V_{\text{ex}} \ll 1$ . When  $\gamma$  approaches unity (Equation 6 is

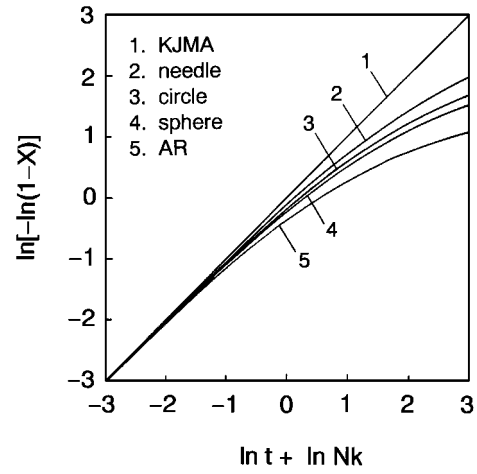


Figure 1 Plots of  $\ln[-\ln(1 - X)]$  versus  $\ln t$  at a constant nucleation rate  $N$  in Equation 5: (1) the KJMA model ( $\gamma = 1$ ); (2) the present model for needle-shaped crystallites in one dimension ( $\gamma = 3/4$ ); (3) the present model for circular crystallites in two dimensions ( $\gamma = 1 - 3^{3/2}/4\pi$ ); (4) the present model for spherical crystallites in three dimensions ( $\gamma = 15/32$ ); (5) the AR model ( $\gamma = 0$ ).

not defined at  $\gamma = 1$ ),  $n$  tends to unity. Hence, the KJMA model is recovered at the beginning of the transformation ( $V_{\text{ex}} \rightarrow 0$ ) or at the KJMA approximation ( $\gamma \rightarrow 1$ ).

When  $\gamma$  is zero, Equation 5 reduces to

$$X_{\text{AR}} = 1 - \frac{1}{1 + V_{\text{ex}}} \quad (7)$$

This is identical to the AR solution; the KJMA plot for  $\gamma = 0$  is equivalent to the KJMA plot of the AR solution.

Plots of  $\ln[-\ln(1 - X)]$  versus  $\ln t$  at a constant nucleation rate  $N$  in Equation 5 are shown in Fig. 1 for three crystallites [12]: needle-shaped crystallites in one dimension ( $\gamma = 3/4$ ); circular crystallites in two dimensions ( $\gamma = 1 - 3^{3/2}/4\pi$ ); and spherical crystallites in three dimensions ( $\gamma = 15/32$ ). The straight line is the result for the KJMA model ( $\gamma = 1$ ) and the lower curve is the result for the AR model ( $\gamma = 0$ ). The slope of  $\ln[-\ln(1 - X)]$  versus  $\ln t$  decreases with decreasing  $\gamma$  and increasing  $t$ .

The values of  $n$  at a constant nucleation rate in Equation 6 are shown in Fig. 2 for the three crystallites. The upper line,  $n = 1$ , is the result for the KJMA model ( $\gamma = 1$ ) and the lower curve is the result for the AR model ( $\gamma = 0$ ). It is clear that the application of the KJMA plot to the present model is inappropriate, except at the beginning of the transformation.

Before turning to a discussion of the evaluation of the present kinetic exponents, a few remarks should be made concerning the AR plot. If the AR model ( $\gamma = 0$ ) were applied, the transformed fraction,  $X_{\text{AR}}$ , would be expressed by Equation 7. At a constant nucleation rate,  $\ln[X_{\text{AR}}/(1 - X_{\text{AR}})]$  versus  $\ln t$  results in a slope of unity. The AR model then yields  $n = 1$  with  $\gamma = 0$ . In other words, a plot of  $\ln[X/(1 - X)]$  versus  $\ln t$  does not result in a straight line in the present model because  $0 < \gamma < 1$ .

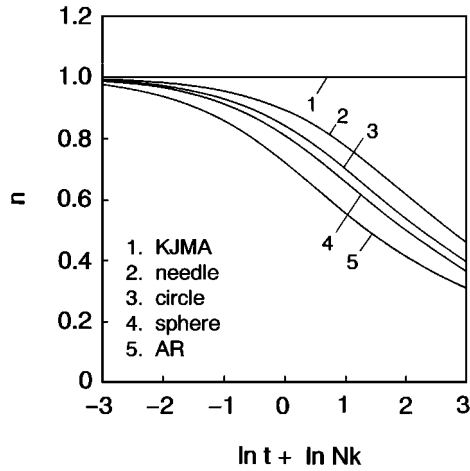


Figure 2 Values of  $n$  in the KJMA plot in Fig. 1: (1) the KJMA model ( $\gamma = 1$ ); (2) the needle-shaped crystallites ( $\gamma = 3/4$ ); (3) the circular crystallites ( $\gamma = 1 - 3^{3/2}/4\pi$ ); (4) the spherical crystallites ( $\gamma = 15/32$ ); (5) the AR model ( $\gamma = 0$ ).

## 2.2. Evaluation of the time exponent and the overlap factor

The time exponent,  $n$ , and the overlap factor,  $\gamma$ , are evaluated without the KJMA plot or the AR plot. Equation 5 is rewritten as

$$D(\gamma) = \ln \left[ \frac{(1 - X)^{\gamma-1} - 1}{1 - \gamma} \right] \quad (8)$$

$$= \ln V_{\text{ex}} \quad (9)$$

When a suitable value of  $\gamma$  is adopted, a plot of  $D(\gamma)$  versus  $\ln V_{\text{ex}}$  leads to a straight line. At a constant nucleation rate,  $N$ , Equation 9 reduces to a form similar to that suggested by Lee and Kim [8]

$$D(\gamma) = \ln t + \ln(kN) \quad (10)$$

Hence, the value of  $\gamma$  in the present model can be obtained by setting a straight line with a slope of unity ( $n = 1$ ).

Plots of  $D(\gamma)$  in Equation 8 versus  $\ln t$  are shown in Fig. 3 for the three crystallites. In this figure, the straight line is set for the circular crystallites ( $\gamma = 1 - 3^{3/2}/4\pi$ ). The other curves thus show the deviations from the straight line on setting different values ( $\gamma = 3/4$  and  $15/32$ ); the deviations become more obvious at the final stage of the transformation. The upper curve shows the result for the AR model ( $\gamma = 0$ ) and the lower curve is for the KJMA model ( $\gamma = 1$ ). As can be seen in Fig. 3, positive deviations occur when lower values of  $\gamma$  are adopted; in contrast, negative deviations occur when higher values of  $\gamma$  are adopted [8].

We can thus estimate the crystal shape and the growth dimension from the value of  $\gamma$  because the mathematical value of  $\gamma$  has already been obtained for several important cases [12].

## 3. Activation energy of nucleation

In the simplest form, the nucleation rate,  $N$ , is only a function of the temperature. Usually  $N$  is assumed to

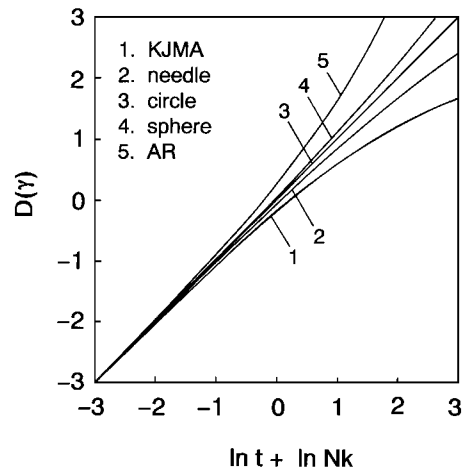


Figure 3 Plots of  $D(\gamma)$  in Equation 8 versus  $\ln t$  at a constant nucleation rate  $N$ : (1) the KJMA model ( $\gamma = 1$ ); (2) the needle-shaped crystallites ( $\gamma = 3/4$ ); (3) the circular crystallites ( $\gamma = 1 - 3^{3/2}/4\pi$ ); (4) the spherical crystallites ( $\gamma = 15/32$ ); (5) the AR model ( $\gamma = 0$ ). The straight line (curve 3) is set for the circular crystallites ( $\gamma = 1 - 3^{3/2}/4\pi$ ); the other curves thus show the deviations from the straight line on setting different  $\gamma$  values.

obey the Arrhenius relation

$$N(T) = N_0 \exp\left(-\frac{Q}{RT}\right) \quad (11)$$

where  $N_0$  is the pre-exponential factor,  $Q$  the activation energy of nucleation,  $R$  the gas constant, and  $T$  the absolute temperature. Under isothermal conditions, the temperature,  $T$ , is independent of time. The kinetic equation is then expressed as

$$\frac{dX}{dt} = kN_0(1 - X)^{2-\gamma} \exp\left(-\frac{Q}{RT}\right) \quad (12)$$

If the KJMA equation ( $\gamma = 1$ ) were applied to the present process, the activation energy,  $Q$ , would be expressed as [20]

$$\frac{Q(t_1)}{R} = - \left\{ \frac{d \ln[-\ln(1 - X)]}{d(1/T)} \right\}_{t_1} \quad (13)$$

If the AR equation ( $\gamma = 0$ ) were applied,  $Q$  would be expressed as [20]

$$\frac{Q(t_1)}{R} = - \left\{ \frac{d \ln[X/(1 - X)]}{d(1/T)} \right\}_{t_1} \quad (14)$$

In the present equation ( $0 < \gamma < 1$ ), the activation energy,  $Q$ , can be expressed as

$$\frac{Q(t_1)}{R} = - \left\{ \frac{d \ln[(1 - X)^{\gamma-1} - 1]}{d(1/T)} \right\}_{t_1} \quad (15)$$

Thus, the activation energy can be obtained from the values of the overlap factor  $\gamma$  and  $X$  taken for reaching a fixed time  $t_1$ , measured at various temperatures. Here Equation 15 agrees with the AR equation (Equation 14) by setting  $\gamma = 0$ . Equation 15 does not agree with the

KJMA equation (Equation 13) in the limit  $\gamma \rightarrow 1$  because Equation 15 is not defined at  $\gamma = 1$ . Therefore, Equation 15 can be applied in the region ( $0 \leq \gamma < 1$ ).

Hillert [20] proposed a more fundamental equation using a fixed transformed fraction  $X_1$ . From Equation 12 the present kinetic equation is rewritten as

$$\ln\left(\frac{dX}{dt}\right)_{X_1} = \ln(kN_0) - \frac{Q^*}{RT} + (2 - \gamma)\ln(1 - X_1) \quad (16)$$

A plot of  $\ln(dX/dt)_{X_1}$  versus  $1/T$  then yields a straight line with a slope of  $-Q^*/R$ . As can be seen from Equation 16, the value of  $Q^*$  is not directly related to  $\gamma$ ; however,  $\gamma$  appears as a constant term in Equation 16.

The integration of Equation 12 is usually used [8, 20] when the measurement of  $X$  results in large uncertainties in evaluating  $(dX/dt)_{X_1}$ . At a fixed transformed fraction,  $X_1$ , we obtain

$$\ln(t)_{X_1} = \frac{Q(X_1)}{RT} + \ln A(X_1) \quad (17)$$

where

$$A(X_1) = \frac{(1 - X_1)^{\gamma-1} - 1}{(1 - \gamma)kN_0} \quad (18)$$

A plot of  $\ln(t)_{X_1}$  versus  $1/T$  produces a straight line with a slope of  $Q/R$ .

The activation energy,  $Q^*$ , in Equation 16 is an instantaneous value at  $X_1$ . In contrast,  $Q$  in Equation 17 is the mean value of  $Q^*$  from the beginning of the transformation to  $X_1$ . It has been reported [8, 20] that the two activation energies  $Q^*$  and  $Q$  are identical when they are independent of the transformed fraction,  $X$ .

#### 4. Conclusion

Methods for determining the kinetic exponents in the equation used for the nucleation and half-in-growth process, have been presented. This equation is given by  $dX/dV_{\text{ex}} = (1 - X)^{2-\gamma}$ , where  $X$  is the transformed fraction,  $V_{\text{ex}}$  is the KJMA extended volume fraction, and  $\gamma$  is the overlap factor to account for the probability of the overlap between a crystallite and a phantom crystallite. The applications of the KJMA plot

( $\gamma = 1, n = 1$ ) and the AR plot ( $\gamma = 0, n = 1$ ) are inappropriate, because the overlap factor is  $0 < \gamma < 1$  in the present process.

The linear relation of  $\ln\{[(1 - X)^{\gamma-1} - 1]/(1 - \gamma)\}$  versus  $\ln t$  has been used to determine the impingement exponent ( $2 - \gamma$ ) and the time exponent ( $n = 1$ ). Deviations from the straight line on setting different values of  $\gamma$  become more obvious at the final stage of the transformation. The crystal shape and growth dimension can thus be estimated by referring to the mathematical value of  $\gamma$ .

The methods of evaluating the activation energy,  $Q$ , have been presented using the Arrhenius relation. The value of  $Q$  is not directly related to  $\gamma$ ; however,  $\gamma$  appears as a constant term in the expression for  $Q$ .

#### References

1. A. N. KOLMOGOROV, *Izv. Akad. Nauk SSSR Ser. Matemat.* **1** (1937) 355.
2. W. A. JOHNSON and R. F. MEHL, *Trans. Am. Inst. Min. Eng.* **135** (1939) 416.
3. M. AVRAMI, *J. Chem. Phys.* **7** (1939) 1103.
4. *Idem, ibid.* **8** (1940) 212.
5. *Idem, ibid.* **9** (1941) 177.
6. J. B. AUSTIN and R. L. RICKETT, *Trans. Am. Inst. Min. Eng.* **135** (1939) 396.
7. B. S. LEMENT and M. COHEN, *Acta Metall.* **4** (1956) 469.
8. E. LEE and Y. G. KIM, *Acta Metall. Mater.* **38** (1990) 1669.
9. H. E. KISSINGER, *Anal. Chem.* **29** (1957) 1702.
10. T. OZAWA, *Bull. Chem. Soc. Jpn.* **38** (1965) 1881.
11. E. LEE and Y. G. KIM, *Acta Metall. Mater.* **38** (1990) 1677.
12. T. TAGAMI and S.-I. TANAKA, *Philos. Mag.* **A74** (1996) 965.
13. *Idem, Appl. Surf. Sci.* **117/118** (1997) 147.
14. *Idem, Acta Mater.* **45** (1997) 3341.
15. *Idem, ibid.* **46** (1998) 1055.
16. P. D. PERSANS, A. RUPPERT and B. ABELES, *J. Non-Cryst. Solids* **102** (1988) 130.
17. T. TAGAMI, Y. WAKAYAMA and S.-I. TANAKA, *Jpn. J. Appl. Phys.* **36** (1997) L734.
18. K. J. CHEN, X. F. HUANG, J. XU, S. YAMASAKI, K. TANAKA, H. KAWANAMI, H. OHEDA AND A. MATSUDA, *J. Non-Cryst. Solids* **164-166** (1993) 977.
19. J. DUTTA, I. M. REANEY, P. ROCA I CABARROCAS and H. HOFMANN, *Nanostruct. Mater.* **6** (1995) 843.
20. M. HILLERT, *Acta Metall.* **7** (1959) 653.

Received 28 May 1997

and accepted 28 July 1998